Preprints of the 19th World Congress
The International Federation of Automatic Control
Cape Town, South Africa. August 24-29, 2014

Performance Limits for Control of Boundary Layer Streaks Induced by Free Stream Turbulence

James F Whidborne * **Liang Lu** ** **George Papadakis** **
Pierre Ricco ***

* *School of Engineering, Cranfield University, Bedfordshire MK45 0AL, UK. email:j.f.whidborne@cranfield.ac.uk*
** *Department of Aeronautics, Imperial College London, London SW7 2AZ, UK. email:g.papadakis@imperial.ac.uk*
*** *Department of Mechanical Engineering, The University of Sheffield, Sheffield S1 3JD, UK. email:p.ricco@sheffield.ac.uk*

Abstract: The problem of controlling boundary layer streaks induced by free stream turbulence for flow over a flat plate is considered. The flow model is expressed in a velocity-pressure form, and analytic expressions of initial and outer boundary conditions can be obtained. From these, a spatially varying linear small perturbation model at a particular wavenumber is obtained for which a control, in the form of wall-normal transpiration, can be applied. Because the initial conditions and disturbances are known, an open-loop optimal control that minimizes the maximum perturbation energy is proposed. Standard minimum sum of square controls are also used. The results provide performance limits for the system as well as potentially providing the basis for a model predictive control scheme.

1. INTRODUCTION

The feedback control of flow fields is a problem that has attracted significant interest over recent years. In particular, the problem of controlling the boundary layer of a spatially developing flow is of importance for drag reduction on air and marine craft. The main objective of the control is prevent the flow becoming turbulent and so maintain the flow as laminar. For flow over a flat plate there are essentially two mechanisms causing a transition from a laminar flow to turbulence. The first generally occurs when the freestream turbulence is low and background noise (resulting from wall roughness, wall vibrations as well as free-stream vortical, acoustic and entropy perturbations) excites boundary layer instability modes such as Tollmien-Schlichting waves. The second, known as bypass transition, occurs when free-stream perturbations are relatively high and longitudinal vortices/streaks interact with the boundary layer leading to unstable environment which leads to the onset of turbulence. This flow scenario is very common over turbine blades and in other industrial internal flows.

A common measure of the system sensitivity for flow field control problems is the transient energy growth [Reddy and Henningson, 1993, Bewley and Liu, 1998, Schmid and Henningson, 2001, for example]. The transient energy perturbations is the square of the (appropriately weighted) Euclidian distance of the state of the linearized system from the origin. The transient energy growth is the maximum energy following an initial unit energy state perturbation. Hence for fluid flow control systems, a useful control objective is the minimization of the maximum transient energy growth of the flow perturbations [Bewley and Liu, 1998, Zhao and Bau, 2006, Whidborne and McKernan, 2007, Whidborne et al., 2008, for example].

The problem of the feedback control of the streaky structures via active-wall transpiration has been the subject of a recent study by Lu and Papadakis [2014], also see Lu et al. [2014]. In this study, the freestream vortical perturbation which generates the streaks inside the boundary layer is rigourously accounted for. Other models that describe the streaks instead completely neglect the freestream perturbation [Luchini, 2000, Andersson et al., 1999, for example]. An outline is given in Section 2, where a finite-dimension state-space model is developed based on a velocity-pressure formulation. The model is discretized in the streamwise direction, and formulated such that the independent variable is the streamwise distance. This results in a linear spatially varying model (or, more generally, a linear sample varying model) with known disturbances and initial condition. A two degree-of-freedom linear spatially varying controller that minimizes a cost function that is a traditional sum of the transient energy over the spatial domain is used. This requires the solution of an algebraic Riccati equation at each point in the streamwise direction.

Since the initial condition and external perturbation are known, the optimal control can be calculated by solving in an open-loop optimal control problem. This is relatively straightforward from a mathematical perspective for a stable linear system. Of course, the system is subject to unknown perturbations and disturbances and hence this approach is not suitable for practical implementation. What the open-loop optimal control does provide is the limit of performance of any closed-loop scheme. Furthermore, to account for the unknown perturbations and disturbances,

⋆ This work was supported by EPSRC grant number EP/I016090/1.

the control could be implemented in a model predictive control fashion [Kothare et al., 1996, Maciejowski, 2002].

Hence this paper investigates the open-loop optimal control of boundary layer streaks. The next section gives an overview of the derivation of a linear spatially varying model developed by Lu and Papadakis [2014], this is based on the work of [Leib et al., 1999] where fuller details and definitions can be found. The control problems are defined and solutions proposed in Section 3. The results of the optimal control solutions are also presented in Section 4. Finally some conclusions are drawn along with a discussion of potential future work to extend to an MPC scheme.

2. FLOW MODEL

Consider a flow of uniform velocity, U_∞, over an infinitely-thin flat plate due to a homogeneous, statistically-stationary turbulence field. The purely convected perturbations are passively advected by the mean flow. In this paper, the flow is described in terms of a Cartesian coordinates system, in which a point can be represented as a position vector $[x, y, z]$, where x, y and z define the streamwise, wall-normal and spanwise directions, respectively. These coordinates are non-dimensionalised by Λ, the spanwise integral length scale of the free-stream turbulence. The velocity and pressure are made dimensionless by U_∞ and ρU_∞^2, respectively, where ρ is the constant free-stream fluid density. Time is normalized with Λ/U_∞. The parameter ϵ is a measure of the turbulence intensity.

Since turbulence in the free-stream is assumed to be of low intensity, it can be treated as a linear perturbation about the mean flow and subsequently the scaled turbulence velocity can be represented as a superposition of harmonic disturbances of the form [Leib et al., 1999]

$$\epsilon \boldsymbol{u}_\infty(x-t, y, z) = \epsilon \hat{\boldsymbol{u}}^\infty e^{i(\boldsymbol{k}\cdot\boldsymbol{x} - k_1 t)} \tag{1}$$

where i is the imaginary number, and from the continuity equation we have

$$\hat{\boldsymbol{u}}^\infty \cdot \boldsymbol{k} = 0 \tag{2}$$

where $\hat{\boldsymbol{u}}^\infty = \{\hat{u}_1^\infty, \hat{u}_2^\infty, \hat{u}_3^\infty\}$ and $\boldsymbol{k} = \{k_1, k_2, k_3\}$, k_1, k_2 and k_3 are the streamwise, wall-normal and spanwise wavenumbers, respectively.

We suppose that the turbulent Reynolds number is defined as $r_t = \epsilon R_\Lambda$, where $R_\Lambda \equiv U_\infty \Lambda/\nu$ is the ordinary Reynolds number based on Λ, and ν is the kinematic viscosity of the fluid in the free-stream. When R_Λ is taken to be asymptotically large, the flow domain can be divided into four asymptotic regions [Goldstein, 1997] as shown in Figure 1.

Region I is a primarily inviscid region which has $\mathcal{O}(\Lambda)$ dimensions surrounding the leading edge of the plate. The disturbances in this region are small and they can be treated as linear perturbations about the uniform flow.

Region II is a viscous region underneath region I. The unsteady perturbations in this region are governed by the Linearised Unsteady Boundary-Layer (LUBL) equations [Goldstein, 1997, Leib et al., 1999]. The mean boundary layer is governed by the Blasius equation and the solution in region II is given in Leib et al. [1999].

The perturbation solution in region II is determined by the LUBL equations [Leib et al., 1999] with no-slip boundary

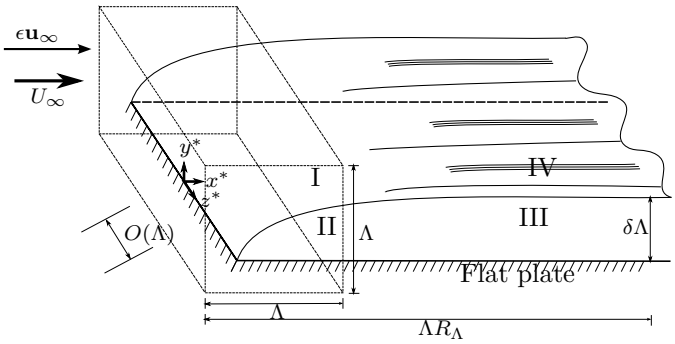

Fig. 1. Flow configuration illustrating the asymptotic structure [Lu and Papadakis, 2014]

conditions at the wall. The solutions of the LUBL equations can be divided into two parts Gulyaev et al. [1989], of which the part involving the velocity perturbation vector, $\{\bar{u}, \bar{v}, \bar{w}\}$, dominates and is used as the upstream condition of the solutions in region III.

The solution in region II becomes invalid when the thickness of boundary layer becomes of the order of the spanwise length scale which takes us into region III. The dominant component solution can be obtained from the linearised Navier-Stokes equations in the form

$$-i\bar{u} + F'\frac{\partial \bar{u}}{\partial \bar{x}} - \frac{F}{2\bar{x}}\frac{\partial \bar{u}}{\partial \eta} - \frac{1}{2\bar{x}}\eta F''\bar{u} + F''\bar{v} = \frac{1}{2\bar{x}}\frac{\partial^2 \bar{u}}{\partial \eta^2} - \kappa^2\bar{u}, \tag{3}$$

$$-i\bar{v} + F'\frac{\partial \bar{v}}{\partial \bar{x}} - \frac{F}{2\bar{x}}\frac{\partial \bar{v}}{\partial \eta} - \frac{1}{4\bar{x}^2}\left(\eta(\eta F')'\bar{u} - F\right)\bar{u} - \frac{1}{2\bar{x}}\eta(\eta F')'\bar{u} = -\frac{1}{2\bar{x}}\frac{\partial \bar{p}}{\partial \eta} + \frac{1}{2\bar{x}}\frac{\partial^2 \bar{v}}{\partial \eta^2} - \kappa^2\bar{v}, \tag{4}$$

$$-i\bar{w} + F'\frac{\partial \bar{w}}{\partial \bar{x}} - \frac{F}{2\bar{x}}\frac{\partial \bar{w}}{\partial \eta} = \kappa^2\bar{p} + \frac{1}{2\bar{x}}\frac{\partial^2 \bar{w}}{\partial \eta^2} - \kappa^2\bar{w}, \tag{5}$$

$$\frac{\partial \bar{u}}{\partial \bar{x}} - \frac{\eta}{2\bar{x}}\frac{\partial \bar{u}}{\partial \eta} + \frac{\partial \bar{v}}{\partial \eta} + \bar{w} = 0, \tag{6}$$

where F is the Blasius function, $\eta = y\sqrt{R_\Lambda/(2x)}$ is a similarity variable, $\bar{x} = k_1 x$ is a scaled streamwise variable [Leib et al., 1999] and $\kappa := k_3/\sqrt{k_1 R_\Lambda}$ is the scaled streamwise wavenumber with $k_1 > 0$. Equations (3) - (6) are called the Linearised Unsteady Boundary-Region (LUBR) equations [Lu and Papadakis, 2014] and correspond to a rational asymptotic limit of the Navier-Stokes equations for low frequency and streamwise-elongated disturbances [Leib et al., 1999]. The equations are solved by using the given upstream and far-field boundary conditions. The condition of upstream boundary is provided by the three-dimensional component of the LUBL equations in region II. The far-field boundary condition can be derived as $\eta \to \infty$ by considering the flow in region IV. The conditions are given by Leib et al. [1999].

The set of LUBR equations, (3)–(6), represent a system of linear PDEs. To obtain the solutions they must be discretised in space in order to get a system with a finite number of state variables and so provide an approximate solution. Spectral collocation and finite difference discretisation methods are used.

The variation of solution in the spanwise direction is approximated by Fourier series. The LUBR equations derived above are based complex perturbation variables $\bar{u}$, $\bar{v}$, $\bar{w}$ and $\bar{p}$ of two dimensions, $\bar{x}$ and η which describe the streamwise and wall-normal directions for a particular given frequency and spanwise wavelength. The Fourier transform in the spanwise direction enables a separate controller to be designed for every independent wavenumber. The individual Fourier modes can be investigated and also they can be superimposed for the whole wavenumber spectrum.

In the wall-normal direction, the distributions of $\bar{u}$, $\bar{v}$, $\bar{w}$, $\bar{p}$ are projected into a series of rational Chebyshev polynomials [Boyd, 2001]. The Chebyshev polynomials series do not make an assumption of periodicity and they have a higher clustering of grid points in the boundary layer compared to Fourier series. The form of Chebyshev polynomials is

$$\Gamma_n(y) = \cos(n \arccos(y)) \tag{7}$$

where $-1 \leq y \leq 1$. The equations are expressed at a grid of Chebyshev collocation points, y_k, where

$$y_k = \cos(\pi k/N), \quad k = 0, \ldots, N. \tag{8}$$

To map the domain $[-1, 1]$ to the domain of the boundary layer, $\eta \in [0, \eta_{\max}]$ we use the mapping proposed by Jones et al. [2011] that is suitable for semi-infinite domains and clusters the collocation points in the near-wall region:

$$\eta_k = \frac{a(1+y_k)}{(by_k)} \tag{9}$$

where $a = \eta_{\text{mid}}\eta_{\max}/(\eta_{\max} - 2\eta_{\text{mid}})$ and $b = 1 + 2a/\eta_{\max}$.

The variables $\bar{u}$, $\bar{v}$, $\bar{w}$ and $\bar{p}$ are approximated by a finite number of $N+1$ Chebyshev polynomials series as

$$\bar{u}(\bar{x},\eta) = \sum_{n=0}^{N} a_{\bar{u},n}(\bar{x})\Gamma_n(\eta), \quad \bar{v}(\bar{x},\eta) = \sum_{n=0}^{N} a_{\bar{v},n}(\bar{x})\Gamma_n(\eta),$$

$$\bar{w}(\bar{x},\eta) = \sum_{n=0}^{N} a_{\bar{w},n}(\bar{x})\Gamma_n(\eta), \quad \bar{p}(\bar{x},\eta) = \sum_{n=0}^{N} a_{\bar{p},n}(\bar{x})\Gamma_n(\eta).$$

The derivatives of the approximations with respect to η can be obtained by differentiating the Chebyshev polynomials only, for instance

$$\frac{\partial \bar{u}(\bar{x},\eta)}{\partial \eta} = \sum_{n=0}^{N} a_{\bar{u},n}(\bar{x})\Gamma'_n(\eta) \tag{10}$$

The distribution of the variables at the collocation points becomes

$$\begin{pmatrix} \bar{u}(\bar{x},\eta_0) \\ \vdots \\ \bar{u}(\bar{x},\eta_N) \end{pmatrix} = \begin{bmatrix} \Gamma_0(\eta_0) & \cdots & \Gamma_N(\eta_0) \\ \vdots & \ddots & \vdots \\ \Gamma_0(\eta_N) & \cdots & \Gamma_N(\eta_N) \end{bmatrix} \begin{pmatrix} a_{\bar{u},0} \\ \vdots \\ a_{\bar{u},N} \end{pmatrix} \tag{11}$$

and the derivatives become

$$\begin{pmatrix} \bar{u}'(\bar{x},\eta_0) \\ \vdots \\ \bar{u}'(\bar{x},\eta_N) \end{pmatrix} = \begin{bmatrix} \Gamma'_0(\eta_0) & \cdots & \Gamma'_N(\eta_0) \\ \vdots & \ddots & \vdots \\ \Gamma'_0(\eta_N) & \cdots & \Gamma'_N(\eta_N) \end{bmatrix} \begin{pmatrix} a_{\bar{u},0} \\ \vdots \\ a_{\bar{u},N} \end{pmatrix} \tag{12}$$

After the spectral discretization of the LUBR equations in the wall-normal direction, the evaluation of the equations at all the collocation points are obtained and the equations can be assembled into the form

$$\mathbf{L}\frac{d\hat{\mathbf{q}}}{d\bar{x}} = \mathbf{M}\hat{\mathbf{q}} + \mathbf{d} \tag{13}$$

where where vector $\hat{\mathbf{q}}$ is the set of all coefficients of velocity and pressure i.e.

$$\hat{\mathbf{q}} = [a_{\bar{u},0}, \ldots, a_{\bar{u},N}, a_{\bar{v},0}, \ldots, a_{\bar{v},N}, a_{\bar{w},0}, \ldots, a_{\bar{w},N}, a_{\bar{p},0}, \ldots, a_{\bar{p},N}]^T$$

and $\mathbf{L}$, $\mathbf{M}$ contain the coefficients of the unknown variables corresponding to the LUBR equations and $\mathbf{d}$ describes the external forcing from free-stream turbulence and is obtained from the far-field boundary conditions in region IV.

The discretization of the LUBR equations are described in Lu and Papadakis [2014]. The developed set in (13) is parabolic in the streamwise direction, $\bar{x}$. Because the streamwise derivative of pressure does not appear in the equations, all the elements of the corresponding columns for the matrix on the left-hand side are zeros, and it is singular. But by discretizing with a first-order Euler implicit scheme, the system in (13) becomes

$$\left(\frac{\mathbf{L}(i)}{\Delta\bar{x}} - \mathbf{M}(i)\right)\hat{\mathbf{q}}(i+1) = \frac{\mathbf{L}(i)}{\Delta\bar{x}}\hat{\mathbf{q}}(i) + \mathbf{d}(i) \tag{14}$$

where i and $i+1$ denote the values of state variables at positions $\bar{x}(i)$ and $\bar{x}(i+1)$ respectively, and $\Delta\bar{x} = \bar{x}(i+1) - \bar{x}(i)$ is the distance between two consecutive positions and is constant for all i. Now the left-hand side of the system is nonsingular and so the autonomous LTV system is obtained as

$$\hat{\mathbf{q}}(i+1) = \left(\frac{\mathbf{L}(i)}{\Delta\bar{x}} - \mathbf{M}(i)\right)^{-1}\frac{\mathbf{L}(i)}{\Delta\bar{x}}\hat{\mathbf{q}}(i) + \left(\frac{\mathbf{L}(i)}{\Delta\bar{x}} - \mathbf{M}(i)\right)^{-1}\mathbf{d}(i). \tag{15}$$

The system can be controlled by applying transpiration at the surface of the plate, which means varying the boundary condition. From the flow system presented in the previous section, we know that the LUBR equations-based system is linear and homogeneous with homogeneous boundary conditions at the wall. With transpiration, the non-zero wall-normal velocity at the wall, $\bar{v}_w$, introduces inhomogeneous boundary condition. Since the system is linear, the homogeneous equations with inhomogeneous boundary conditions can be transformed into inhomogeneous equations with homogeneous boundary conditions. The state vector $\hat{\mathbf{q}}$ can be obtained as the sum of two parts: $\mathbf{q}_h$, the solution of the homogeneous problem with homogeneous boundary condition and $\mathbf{q}_p$, the solution of the homogeneous problem with inhomogeneous boundary condition [Högberg and Henningson, 2002]. It can be expressed as

$$\hat{\mathbf{q}} = \mathbf{q}_h + \bar{v}_w(\bar{x})\mathbf{q}_p \tag{16}$$

where $\bar{v}_w(\bar{x})$ is the streamwise dependent wall-normal velocity and $\mathbf{q}_p$ is the particular solution of homogeneous system when the wall-normal velocity is set as $\bar{v}_w(\bar{x}) = 1$. With the discretization schemes described earlier for the uncontrolled case, the system can be expressed in the form of (17) that is used next.

3. CONTROL METHOD

3.1 Model Description

The system description considered is linear sample varying systems with a known state disturbance. This descrip-

tion also includes linear discrete-time varying and linear discrete-time invariant system models. The state space description is given by

$$\hat{\mathbf{q}}(k+1) = \mathbf{A}(k)\hat{\mathbf{q}}(k) + \mathbf{d}(k) + \mathbf{B}(k)\mathbf{u}(k) \tag{17}$$

where $k = 0, 1, \ldots, n$ is the sample index number, $\mathbf{A}(k) \in \mathbb{R}^{p\times p}$ is the state matrix at the kth sample, $\mathbf{B}(k) \in \mathbb{R}^{p\times m}$ is the input matrix, $\hat{\mathbf{q}}(k) \in \mathbb{R}^p$, $\mathbf{u}(k) \in \mathbb{R}^m$ and $\mathbf{d}(k) \in \mathbb{R}^p$ denote the state vector, control variable and state disturbance respectively.

Let the initial condition, $\hat{\mathbf{q}}(0)$, disturbance, $\mathbf{d} = [\mathbf{d}^T(0), \mathbf{d}^T(1), \ldots, \mathbf{d}^T(n)]^T$ and control, $\mathbf{u} = [\mathbf{u}^T(0), \mathbf{u}^T(1), \ldots, \mathbf{u}^T(n)]^T$ be known. Then the solution to (17) is given by

$$\begin{aligned}
\hat{\mathbf{q}}(1) &= \mathbf{A}(0)\hat{\mathbf{q}}(0) + \mathbf{d}(0) + \mathbf{B}(0)\mathbf{u}(0)\\
\hat{\mathbf{q}}(2) &= \mathbf{A}(1)\hat{\mathbf{q}}(1) + \mathbf{d}(1) + \mathbf{B}(1)\mathbf{u}(1)\\
&= \mathbf{A}(1)\mathbf{A}(0)\hat{\mathbf{q}}(0) + \mathbf{A}(1)\mathbf{d}(0) + \mathbf{d}(1)\\
&\quad + \mathbf{A}(1)\mathbf{B}(0)\mathbf{u}(0) + \mathbf{B}(1)\mathbf{u}(1)\\
&= \Phi(1,0)\hat{\mathbf{q}}(0) + \Phi(1,1)\mathbf{d}(0) + \mathbf{d}(1)\\
&\quad + \Phi(1,1)\mathbf{B}(0)\mathbf{u}(0) + \mathbf{B}(1)\mathbf{u}(1)\\
&\ \ \vdots \quad \vdots \quad \vdots\\
\hat{\mathbf{q}}(n) &= \Phi(n-1,0)\hat{\mathbf{q}}(0) + \Phi(n-1,1)\mathbf{d}(0)\\
&\quad + \Phi(n-1,2)\mathbf{d}(1) + \ldots + \mathbf{d}(n-1)\\
&\quad + \Phi(n-1,1)\mathbf{B}(0)\mathbf{u}(0) + \Phi(n-1,2)\mathbf{B}(1)\mathbf{u}(1) + \ldots\\
&\quad \ldots + \mathbf{B}(n-1)\mathbf{u}(n-1)
\end{aligned} \tag{18}$$

where $\Phi(k,j) := \mathbf{A}(k)\mathbf{A}(k-1)\cdots\mathbf{A}(j+1)\mathbf{A}(j)$ for all $k \geq j$. This can be written as

$$\begin{aligned}
\hat{\mathbf{q}}(i) &= \Phi(i-1,0)\hat{\mathbf{q}}(0)\\
&\quad + \sum_{j=1}^{i-1}\Phi(i-1,j)\mathbf{d}(j-1) + \mathbf{d}(i-1)\\
&\quad + \sum_{j=1}^{i-1}\Phi(i-1,j)\mathbf{B}(j-1)\mathbf{u}(j-1) + \mathbf{B}(i-1)\mathbf{u}(i-1)\\
&\qquad\qquad\qquad\qquad \text{for } i = 1, \ldots, n.
\end{aligned} \tag{19}$$

We can also write (18) in matrix-vector form as

$$\begin{bmatrix} \hat{\mathbf{q}}(1)\\ \hat{\mathbf{q}}(2)\\ \vdots\\ \hat{\mathbf{q}}(n-1)\\ \hat{\mathbf{q}}(n)\end{bmatrix} = \begin{bmatrix} \Phi(1,0)\\ \Phi(2,0)\\ \vdots\\ \Phi(n-1,0)\\ \Phi(n,0)\end{bmatrix}\hat{\mathbf{q}}(0)$$
$$+ \begin{bmatrix} I & 0 & 0 & \cdots\\ \Phi(1,1) & I & 0 & \cdots\\ \Phi(2,1) & \Phi(2,2) & I & \cdots\\ \vdots & \vdots & \vdots & \ddots\\ \Phi(n-2,1) & \Phi(n-2,2) & \Phi(n-2,3) & \cdots\\ \Phi(n-1,1) & \Phi(n-1,2) & \Phi(n-1,3) & \cdots \end{bmatrix}$$
$$\begin{bmatrix} \cdots & 0 & 0\\ \cdots & 0 & 0\\ \cdots & 0 & 0\\ \ddots & \vdots & \vdots\\ \cdots & I & 0\\ \cdots & \Phi(n-1,n-1) & I\end{bmatrix}\begin{bmatrix} \mathbf{d}(0)\\ \mathbf{d}(1)\\ \vdots\\ \mathbf{d}(n-2)\\ \mathbf{d}(n-1)\end{bmatrix}$$
$$+ \begin{bmatrix} \mathbf{B}(0) & 0 & 0 & \cdots\\ \Phi(1,1)\mathbf{B}(0) & \mathbf{B}(1) & 0 & \cdots\\ \Phi(2,1)\mathbf{B}(0) & \Phi(2,2)\mathbf{B}(1) & \mathbf{B}(2) & \cdots\\ \vdots & \vdots & \vdots & \ddots\\ \Phi(n-2,1)\mathbf{B}(0) & \Phi(n-2,2)\mathbf{B}(1) & \Phi(n-2,3)\mathbf{B}(2) & \cdots\\ \Phi(n-1,1)\mathbf{B}(0) & \Phi(n-1,2)\mathbf{B}(1) & \Phi(n-1,3)\mathbf{B}(2) & \cdots \end{bmatrix}$$
$$\begin{bmatrix} \cdots & 0 & 0\\ \cdots & 0 & 0\\ \cdots & 0 & 0\\ \ddots & \vdots & \vdots\\ \cdots & \mathbf{B}(n-2) & 0\\ \cdots & \Phi(n-1,n-1)\mathbf{B}(n-2) & \mathbf{B}(n-1)\end{bmatrix}\begin{bmatrix} \mathbf{u}(0)\\ \mathbf{u}(1)\\ \vdots\\ \mathbf{u}(n-2)\\ \mathbf{u}(n-1)\end{bmatrix} \tag{20}$$

where I is the identity matrix of appropriate dimension. This can be written as

$$\hat{\mathbf{q}} = \Psi\hat{\mathbf{q}}(0) + \Upsilon\mathbf{d} + \Xi\mathbf{u} \tag{21}$$

Alternatively, we can write (19) as

$$\hat{\mathbf{q}}(i) = \Psi_i\hat{\mathbf{q}}(0) + \Upsilon_i\mathbf{d}_i + \Xi_i\mathbf{u}_i \quad \text{for } i = 1, \ldots, n \tag{22}$$

where

$$\begin{aligned}
\Psi_i &= \Phi(i-1,0),\\
\Upsilon_i &= [\Phi(i-1,1)\ \Phi(i-1,2)\ \cdots\ \Phi(i-1,i-1)\ I]\\
\Xi_i &= [\Phi(i-1,1)\mathbf{B}\ \Phi(i-1,2)\mathbf{B}\ \cdots\ \Phi(i-1,i-1)\mathbf{B}\ \mathbf{B}]\\
\mathbf{d}_i &= \left[\mathbf{d}^T(0)\ \mathbf{d}^T(1)\ \cdots\ \mathbf{d}^T(i-2)\ \mathbf{d}^T(i-1)\right]^T\\
\mathbf{u}_i &= \left[\mathbf{u}^T(0)\ \mathbf{u}^T(1)\ \cdots\ \mathbf{u}^T(i-2)\ \mathbf{u}^T(i-1)\right]^T
\end{aligned}$$

3.2 Open-loop Optimal Control Problems

Problem 1 The problem is to choose the control $\mathbf{u}$ so as to minimize the effect of a known disturbance $\mathbf{d}$ and initial condition $\hat{\mathbf{q}}(0)$ on the state $\hat{\mathbf{q}}$, or more particularly on the state perturbation energies $\hat{\mathbf{q}}^T(i)Q(i)\hat{\mathbf{q}}(i)$. That is

$$\mathbf{u}_{\min} = \arg\min_{\mathbf{u}} \sum_{i=1}^{n}\hat{\mathbf{q}}^T(i)Q(i)\hat{\mathbf{q}}(i) \tag{23}$$

subject to

$$\hat{\mathbf{q}} = \tilde{\hat{\mathbf{q}}} + \Xi\mathbf{u} \tag{24}$$

where $\tilde{\hat{\mathbf{q}}} = \Psi\hat{\mathbf{q}}(0) + \Upsilon\mathbf{d}$ and $Q(i) = Q(i)^T > 0$ for all i.

This is a standard linear least squares problem that can be solved easily [Boyd and Vandenberghe, 2004, for example]. We rewrite the problem as

$$\mathbf{u}_{\min} = \arg\min_{\mathbf{u}} \phi(\mathbf{u}) \tag{25}$$

where

$$\phi(\mathbf{u}) = \frac{1}{2}\hat{\mathbf{q}}^T\mathbf{Q}\hat{\mathbf{q}} \tag{26}$$

where $\mathbf{Q} := \operatorname{diag}(Q(1), \ldots, Q(n))$. The optimality necessary condition $\partial\phi(\mathbf{u})/\partial\mathbf{u} = 0$ gives

$$\Xi^T\mathbf{Q}\tilde{\hat{\mathbf{q}}} + \mathbf{u}(\Xi^T\mathbf{Q}\Xi) = 0. \tag{27}$$

If Ξ has rank n, then

$$\mathbf{u}_{\min} = -(\Xi^T\mathbf{Q}\Xi)^{-1}\Xi^T\mathbf{Q}\tilde{\hat{\mathbf{q}}} \tag{28}$$

is well-known as the solution.

Problem 2 Now we introduce a cost on the control, so the problem is

$$\mathbf{u}_{\min} = \arg\min_{\mathbf{u}} \left(\hat{\mathbf{q}}^T\mathbf{Q}\hat{\mathbf{q}} + \mathbf{u}^T\mathbf{R}\mathbf{u}\right) \tag{29}$$

where $\mathbf{R}$ is a weighting matrix of appropriate dimensions. The solution is easily found as

$$\mathbf{u}_{\min} = -(\Xi^T \mathbf{Q} \Xi + \mathbf{R})^{-1} \Xi^T \mathbf{Q} \tilde{\hat{\mathbf{q}}} \tag{30}$$

where $\tilde{\hat{\mathbf{q}}} = \Psi \hat{\mathbf{q}}(0) + \Upsilon \mathbf{d}$.

Problem 3 Consider now the problem of minimizing the transient energy

$$\mathbf{u}_{\min} = \arg\min_{\mathbf{u}} \max_{i=1,\ldots,n} \left(\hat{\mathbf{q}}^T(i) Q(i) \hat{\mathbf{q}}(i) \right) \tag{31}$$

subject to

$$\hat{\mathbf{q}}(i) = \tilde{\hat{\mathbf{q}}}(i) + \Xi_i \mathbf{u}_i \quad \text{for } i = 1, \ldots, n \tag{32}$$

where $\tilde{\hat{\mathbf{q}}}(i) = \Psi_i \hat{\mathbf{q}}(0) + \Upsilon_i \mathbf{d}_i$.

This is equivalent to the following problem

$$\min_{\substack{u \in \mathbb{R}^{rm} \\ \lambda > 0}} \lambda \tag{33}$$

$$\text{subject to } \hat{\mathbf{q}}^T(i) Q(i) \hat{\mathbf{q}}(i) < \lambda, i = 1, \ldots, n. \tag{34}$$

The constraint $\hat{\mathbf{q}}^T(i) Q(i) \hat{\mathbf{q}}(i) < \lambda$ is equivalent to the LMI [Maciejowski, 2002, p. 236]

$$\begin{bmatrix} \lambda P(i) & \hat{\mathbf{q}}(i)) \\ \hat{\mathbf{q}}^T(i) & 1 \end{bmatrix} \tag{35}$$

$P(i) = Q^{-1}(i)$, provided $Q(i) > 0$. From (32) this gives the set of LMIs

$$\begin{bmatrix} \lambda P(i) & (\Xi_i \mathbf{u}_i + \tilde{\hat{\mathbf{q}}}(i)) \\ (\Xi_i \mathbf{u}_i + \tilde{\hat{\mathbf{q}}}(i))^T & 1 \end{bmatrix} \tag{36}$$

for $i = 1, \ldots, n$. Such an LMI problem can be easily solved using common packages such as SeDuMi [Sturm, 1999] or the MATLAB Robust Control Toolbox.

If any $Q(i)$ are rank deficient, they can be replaced by $\tilde{Q}(i) = Q(i) + \varepsilon I$ where $\varepsilon \ll 1$. Clearly, as $\varepsilon \to 0$, $\tilde{Q}(i) \to Q(i)$.

4. RESULTS

The values $\eta_{\text{mid}} = 4$ and $\eta_{\max} = 15$ are chosen as they give a good balance between solving the boundary layer accurately and not 'wasting' collocation points in unimportant areas [Lu and Papadakis, 2014]. The accuracy increases with N, a value of $N = 150$ is very accurate [Lu and Papadakis, 2014], but makes the solution of Problem 3 very difficult, so the final model is chosen with 25 Chebyshev Gauss-Lobatto collocation points ($N = 25$). The finite difference dicretization interval is selected as $\Delta\bar{x} = 0.01$, which gives an acceptable accuracy [Lu et al., 2014, Lu and Papadakis, 2014].

The perturbation energy weighting matrices, $Q(i)$ are chosen according to a scheme suggested by Bewley and Liu [1998]. The perturbations in the streamwise component are dominant, hence the perturbation energies of v, w and p are neglected.

The perturbation energy from the known initial condition and the disturbance with no control applied is shown in Figure 2. The maximum perturbation energy is 0.193132×10^{-3}.

The three problems of Section 3.2 are solved with the $N = 25$ model. The result from the solution of Problem 1

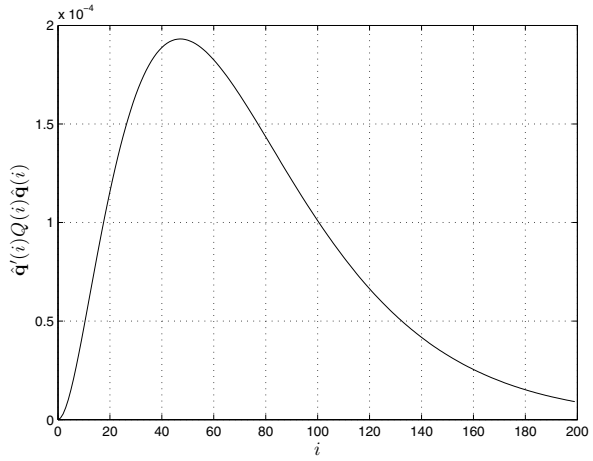

Fig. 2. Uncontrolled perturbation energy

is shown in Figure 3. The maximum perturbation energy is 32.0057×10^{-6}.

Problem 3 was solved using the LMI solver from the MATLAB Robust Control Toolbox. It took several hours to converge to a solution. The maximum perturbation energy is 30.2579×10^{-6} which although is less than for Problem 1, is not significantly less. The difficulty lay in that the perturbations in v, w and p were not included in the perturbation energy measure, hence all the $Q(i)$ are not full rank. Thus to solve Problem 3, $Q(i)$ was replaced by $Q(i) + \epsilon I$ where $\epsilon = 10^{-8}$, this results in sub-optimal solutions. This requires further investigation. The result from the solution of Problem 3 is shown in Figure 3.

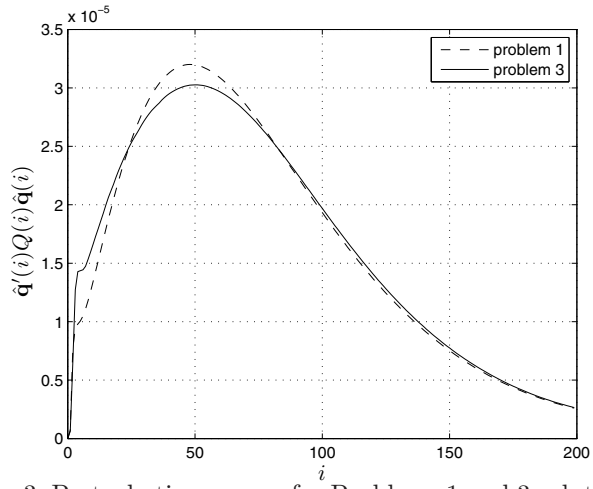

Fig. 3. Perturbation energy for Problems 1 and 3 solutions

The optimal solution control energies, $\mathbf{u}(i)^T \mathbf{u}(i)$, are shown in Figure 4. Clearly, Problem 3 requires greater control. To trade-off the control energy against the performance, Problem 2 is solved for a range of control weightings, $\mathbf{R} = \alpha I$, $\alpha = 10^{-6}, 10^{-5}, \ldots, 1$, the resulting range of perturbation energies are shown in Figure 5 along with the perturbation energy for Problem 1 (dashed line). Note that the perturbation energy for $\alpha = 1$ is almost coincident with the open-loop response of Figure 2. The corresponding maximum perturbation energies and maximum control energies are shown in Table 1.

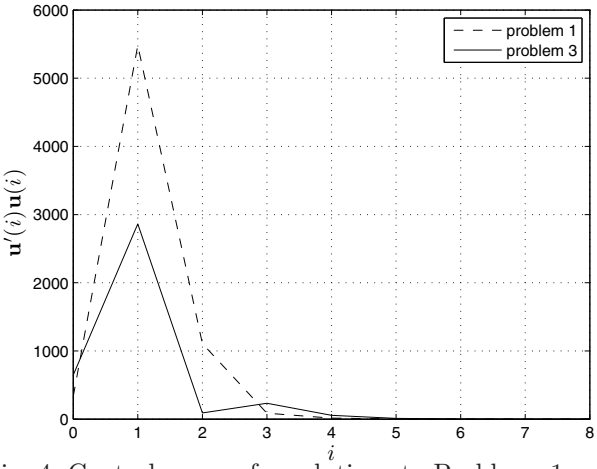

Fig. 4. Control energy for solutions to Problems 1 and 3

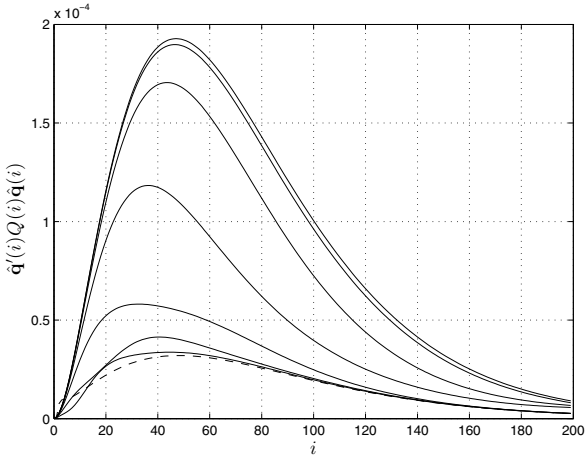

Fig. 5. Perturbation energy for Problem 2 solutions for $\alpha = 10^{-6}, 10^{-5}, \ldots, 1$

Table 1. Maximum perturbation and control energy for Problem 2 with range of weighting α

α	$\max_i(\hat{\mathbf{q}}(i)^T Q(i)\hat{\mathbf{q}}(i))$	$\max_i(\mathbf{u}(i)^T\mathbf{u}(i))$
10^{-6}	33.701×10^{-6}	41.567
10^{-5}	41.396×10^{-6}	8.153
10^{-4}	58.108×10^{-6}	1.192
10^{-3}	118.292×10^{-6}	0.101
10^{-2}	170.503×10^{-6}	4.331×10^{-3}
10^{-1}	189.765×10^{-6}	74.858×10^{-6}
1	192.778×10^{-6}	0.808×10^{-6}

5. CONCLUSIONS

The paper considers the limits of performance for the control of boundary layer streaks by means of wall transpiration. The optimal performance for a known initial condition and disturbance can be calculated by solving three open-loop optimal control problems. The maximum energy perturbation can be minimized by solving a set of LMIs (Problem 3). However this method is computationally expensive. A less computationally expensive method is to minimize the sum of the energy perturbations at each discretization point in the streamwise direction (Problem 1). This results in a 5.8% increase in the resulting maximum energy perturbation over Problem 3, which although significant, is not too great.

Model predictive (or receding horizon control) is a common strategy for implementing the solution of open-loop control problems in a feedback manner so as to account for the uncertainties in system and disturbances that are inevitable in every real-world application. It is envisaged that the open-loop optimal solutions proposed here could be used as a basis for a model predictive approach, the only difference being the terminal point is constant, that means that the horizon approaches as the control steps through in k.

REFERENCES

P. Andersson, M. Berggren, and D. S. Henningson. Optimal disturbances and bypass transition in boundary layers. *Phys. Fluids*, 11:134–150, 1999.

T. R. Bewley and S. Liu. Optimal and robust control and estimation of linear paths to transition. *J. Fluid Mech.*, 365:305–349, 1998.

J. P. Boyd. *Chebyshev and Fourier Spectrum Methods*. Dover, New York, NY, 2nd edition, 2001.

S. Boyd and L. Vandenberghe. *Convex Optimization*. Cambridge University Press, Cambridge, U.K., 2004. ISBN 0521833787.

M. E. Goldstein. Response of the pre-transitional laminar boundary layer to free stream turbulence. *Otto Laporte Lecture. Bull. Am. Phys. Soc.*, 42:2150, 1997.

A. N. Gulyaev, V. E. Kozlov, V. R. Kuznetsov, B.I. Mineev, and A. N. Sekundov. Interaction of a laminar boundary layer with external turbulence. *Fluid Dynamics*, 24(5):700–710, 1989. doi: 10.1007/BF01051722.

M. Högberg and D. S. Henningson. Linear optimal control applied to instabilities in spatially developing boundary layers. *J. Fluid Mech.*, 470:151–179, Nov 2002.

B. L. Jones, E. C. Kerrigan, J. F. Morrison, and T. A. Zaki. Flow estimation of boundary layers using DNS-based wall shear information. *Int. J. Control*, 84:1310–1325, 2011. doi: 10.1080/00207179.2011.593000.

M. V. Kothare, V. Balakrishnan, and M. Morari. Robust constrained model predictive control using linear matrix inequalities. *Automatica*, 32(10):1361–1379, 1996.

S. J. Leib, D. W. Wundrow, and M. E. Goldstein. Effect of free-stream turbulence and other vortical disturbances on laminar boundary layer. *J. Fluid Mech.*, 380:169–203, 1999.

L. Lu and G. Papadakis. Control of streaks induced by free-stream turbulence in incompressible boundary layer: application for linearised model. 2014. Under preparation.

L. Lu, L. Agostini, P. Ricco, and G. Papadakis. Optimal state feedback control of streaks and Gortler vortices induced by free-stream vortical disturbances. In *Proc. 2014 UKACC 10th International Conference on Control (CONTROL 2014)*, Loughborough, U.K., July 2014.

P. Luchini. Reynolds-number-independent instability of the boundary layer over a flat surface: optimal perturbations. *J. Fluid Mech.*, 404:289–309, 2000. doi: 10.1017/S0022112099007259.

J. M. Maciejowski. *Predictive Control with Constraints*. Prentice Hall, Harlow, UK, 2002.

S. C. Reddy and D. S. Henningson. Energy growth in viscous channel flows. *J. Fluid Mech.*, 252:209–238, 1993.

P. J. Schmid and D. S. Henningson. *Stability and Transition in Shear Flows*, volume 142 of *Applied Mathematical Sciences*. Springer, New York, 2001.

J. F Sturm. Using SeDuMi 1.02, a MATLAB toolbox for optimization over symmetric cones. *Optimization Methods and Software*, 11–12 (1–4):625–653, 1999.

J. F. Whidborne and J. McKernan. On the minimization of maximum transient energy growth. *IEEE Trans. Autom. Control*, 52 (9):1762–1767, September 2007. doi: 10.1109/TAC.2007.900854.

J. F. Whidborne, J. McKernan, and G. Papadakis. Minimising transient energy growth in plane Poiseuille flow. *Proc. IMechE J. Syst. Contr. Eng.*, 222(5):323–331, 2008. doi: 10.1243/09596518JSCE493.

H. Zhao and H. H. Bau. Limitations of linear control of thermal convection in a porous medium. *Phys. Fluids*, 18(7), 2006. Art. No. 074109.